Supporting Materials

Solvent-Washable Polymer Templated Synthesis of Mesoporous Materials and Solid-Acid Nanocatalysts in One-Pot

Richard E. Mishler II,[a] Ankush V. Biradar,[a] Cole T. Duncan,[a] Eric A. Schiff,[b,*] and Tewodros Asefa[a,*]

[a] Department of Chemistry, 111 College Place, Syracuse University, Syracuse NY 13244

[b] Department of Physics, Syracuse University, Syracuse, NY 13244

Corresponding Authors: tasefa@syr.edu (T.A.); easchiff@syr.edu (E.A.S.)

Fax: 1-315-443-4070 (T.A.); Tel: 1-315-443-3360 (T.A.); Fax: 1-315-443-9103; Tel: 1-315-443-2566;

Experimental Section

Materials and Reagents

Poly(ethylene glycol)-*block*-poly(propylene glycol)-*block*-poly(ethylene glycol) with number-average molecular weight 5,800 g/mol (P123) and tetraethyl orthosilicate (TEOS) were obtained from Sigma-Aldrich. Dimethyl phosphite (DMP) was purchased from Fluka. Hydrochloric acid (12 M), absolute anhydrous ethyl alcohol (200 proof), acetone, methanol, and diethyl ether, and toluene were obtained from Fisher Scientific.

Synthesis of Phosphonated Tri-Block P123 Copolymer (P123^P)

5.0 g of P123 and 100 mL of DMP were mixed in a 250 mL three-necked flask equipped with a magnetic stirrer and attached to a condenser and refluxed at 150 °C under nitrogen for 4 h. Using a condensation trap, the methanol produced in the reaction was removed. The removal of methanol was also measured to show the progression of the reaction. After the reaction and distillation, the mixture was cooled under nitrogen to room temperature and the unreacted DMP was removed using vacuum, producing a waxy residue of phosphonated pluronics (P123^P) triblock copolymer.

The synthesis of the phosphonated pluronics template, P123^P, was proved by ^{1}H and ^{31}P NMR spectroscopy (Figures S4-7)[1] and gel permeation chromatography (GPC) (Figure S8). ^{1}H NMR (CDCl3): δ 6.75 (d, [1]J(P,H) = 710.12 Hz, CH$_3$OP(O)(*H*)O-); 4.03 (-OP(O)(H)OC*H$_2$*), 4.03 (-OP(O)(H)OC*H$_3$*), and 3.47-3.60 (m, -OC*H$_2$*CH$_2$O-). ^{31}P NMR (CDCl$_3$): δ 11.87-11.91 (m, -CH$_2$O*P*(O)(H)OCH$_3$) and 12.45 (m, residual DMP, CH$_3$O*P*(O)(H)OCH$_3$). The ^{1}H NMR spectra after the reaction between P123 and dimethyl phosphite (DMP) shows a doublet centered at δ 6.75 (d, [1]J(P,H) = 710.12) corresponding to CH$_3$OP(O)(*H*)O-. Furthermore, peaks at δ 4.03 corresponding to -

OP(O)(H)OCH_2- and -OP(O)(H)OCH_3), and 3.47-3.60 (m, -OCH_2CH_2O-) are observed. A peak at 4.01

is missing on the spectrum for P123. This strongly supports the addition of phosphate ester group to the

terminal ends of the PEG of the P123 triblock copolymer. Additionally, the ^{31}P NMR spectrum shows δ

11.87-11.91 corresponding to -CH_2OP(O)(H)OCH_3 and 12.45 corresponding to residual DMP,

CH_3OP(O)(H)OCH_3). The signal at 11.87-11.91 is generated by phosphorous groups attached to the

ends of the P123^P tri-block copolymer. Both the ^{1}H and ^{31}P confirmed the exchange of terminal OH

groups in the PEO template of P123 to phosphate groups (Figures S1-S4). The latter is further

confirmed by running the ^{31}P NMR of pure DMP, which shows a peak at ~ 12.41 ppm. Furthermore, the

polymer was characterized by gel permeation chromatography (GPC) (Figure S5).

Synthesis of Mesoporous Silica with Phosphonated Pluronics, P123^P

SBA-15 type mesoporous material by using phosphonated pluronics, P123^P, as a template was

synthesized by following the procedure reported by Stucky et al.[2] with a minor modification. Typically,

4.15 g of the P123^P template was mixed into and 200.0 mL distilled water under stirring. Upon complete

dissolution of the triblock copolymer, 40.0 mL, 12 M HCl and18.22 g of tetraethyl orthosilicate (TEOS)

were added and the reaction mixture was stirred at 40°C for 20 h. Then the material was aged for 24 h at

80°C. The solution was filtered and the solid product was dried at 90°C for 24 h. This produced the

sample labeled as-synthesized mesostructured material, SBA15^P (The characterization of all the

mesoporous materials are given in Figures 1, 2, and Figures S6 - S10).

Synthesis of Mesoporous Silica SBA-15 with Pluronics, P123

As a control sample, SBA-15 (or labeled here as SBA15), was prepared by following the procedure

reported by Stucky and co-workers.[2] Typically, 4.15 g of the P123 template was mixed with 40.0 mL,

12 M HCl and 200.0 mL distilled water. Upon complete dissolution of the triblock copolymer, 18.22 g

of tetraethyl orthosilicate (TEOS) was added and the reaction mixture was stirred at 40°C for 20 h. Then

the material was aged for 24 h at 80°C. The solution was filtered and the solid product was washed with

copious amount of water and dried at 90°C for 24 h. This produced the sample labeled as-synthesized

mesostructured material, SBA-15 (also denoted here SBA15).

Additionally, samples with lower TEOS:P123^P were synthesized by using 5 g P123^P and 12 g

TEOS (See Figure S8).

Extraction of Template

(A) Solvent washing: 1.0 g of the mesostructured material, SBA15^P or SBA15, synthesized above

was stirred in a 1:1:1 ratio of acetone, ethanol and diethyl ether at 50 °C for 24 h followed by 3 washes

with 20 mL of ethanol and then filtered and dried for 24 h at 80°C. The resulting solvent washed

mesoporous materials synthesized from P123^P and P123 were labeled as SBA15^P-sw and SBA15-sw,

respectively.

(B) Calcination: 1.0 g of the mesostructured material, SBA15^P or SBA15, was kept on a quartz boat

in a quartz cylinder inside a furnace and heated at a ramp of 2.0 °C/min at 600°C for 24 h under air.

Then the heat was ramped down at a rate of 2.0°C/min until the furnace reached room temperature. This

resulted in calcined samples, SBA15^P-cal and SBA15-cal, respectively.

**Solid-Acid Catalyzed Pinacole - Pinacolone Rearrangement Reaction by Phosphonic Acid
Functionalized Mesoporous Catalyst**

A solid acid catalyzed pinacole-pinacolone reaction was conducted by using the mesoporous

material, SBA15^P-sw, as a catalyst. Typically, 0.1 g of benzopinacol was mixed and stirred with 0.1 g

SBA15[P]-sw catalyst and 10.0 mL of toluene at 80 °C. Samples were collected at 0, 6, 12 and 24 h after starting the reactions for three separate runs using the same catalyst to show recyclability. Three different temperatures (80, 100, and 120°C) were also tried close the boiling point of solvent used (toluene ~ 110°C) to determine the most efficient temperature for the transformation of benzopinacol into benzopinacolone. Control experiment using SBA15 as a catalyst was also conducted in the same way. The reaction mixture was taken with a filter syringe and characterized by ^{1}H NMR spectroscopy (Figures S11 - S14).

The ^{1}H NMR spectra of the reaction mixture clearly show that the material synthesized from the phosphonated template after solvent washing, SBA15[P], display solid acid catalytic property for the pinacole – pinacolone transformation as observed in Table 1. In the NMR data for benzopinacol and benzopinacolone Figures S11 and S12 differences in peak shifts can be used to determine the differences and using the integration of peaks a percentage of conversion between the starting material and the product can be determined. The catalyst resulted in ~100% conversion and recyclability.

In Figure S3, when going from A to D, the relative peak intensity of the peak at 3.02 ppm slowly disappeared and a strong peak at ~ 7.8 ppm corresponding to benzopinacolone appeared. This transition from (A) to (D) clearly shows that the pinacole to pinacolone rearrangement is catalyzed by the solid acid catalyst.

Characterization

Solution phase ^{1}H-NMR spectra was measured with a Bruker DPX-300 MHz spectrometer using CDCl$_3$. Solution phase ^{31}P NMR spectra was measured using a Bruker DRX-500 MHz spectrometer. Thermogravimetric analysis (TGA) traces were recorded using Q500 thermogravimetric analyzer (TA Instruments) with temperature ramp at 10 °C/min under air flow. The nitrogen adsorption isotherms, surface area and pore size distributions were measured with a Micromeritics Tri-Star 3000 surface area

and porosity analyzer. The data was calculated by using the Burunauer-Emmett-Teller (BET) and Barrett-Joyner-Halenda (BJH) methods. The transition electron micrographs were taken using the FEI Tecnai T-12 transition electron microscope. FT-IR spectra were obtained with Nicolet 6700 FT-IR spectrometer.

Additional Results and Discussion

FT-IR Spectral Analysis of the Samples

The SBA15 and SBA15^P after solvent washing and calcination were also characterized by FT-IR spectroscopy (Figure S6). The FT-IR spectra of all the mesoporous samples show three peaks at 452-457, 797, and 1070 cm^{-1} corresponding to rocking, bending (or symmetric stretching), and asymmetric stretching of the tetrahedral oxygen atoms in the SiO_2 structure or Si–O–Si framework. A peak at 950 cm^{-1} can be assigned to the asymmetric stretching of silanol, Si-OH, as well as P-OH groups and P-O-P units.[3-5] This peak was slightly broader on the spectrum of sample SBA15^P-sw compared to that of SBA15-sw indicating that the peak may also contain the asymmetric stretching vibrations of P-OH groups and P-O-P units in the latter. The corresponding peak on the spectrum for SBA15^P-cal is prominent and shifted to 975 cm^{-1} compared to that of SBA15^P-sw, indicating that most of the P-OH groups may have been condensed into P-O-Si unites in the former. Additionally, this peak is not observed on the spectrum for SBA15-sw. The peak at 820 cm^{-1} was also observed only on the spectrum of the calcined SBA15^P-cal sample, which corresponds to symmetric stretching of P–O–Si and P-O-P units.

More interestingly, the FTIR spectra of the samples made from phosphonated template exhibited more or stronger peaks in the region of 1150-1300 cm^{-1} compared to the spectra of the samples made

from non-phosphoanted pluronic template. These new peaks are stronger on the spectrum of SBA15[P]-cal compared to that of SBA15[P]. On the other hand, the FT-IR spectra indicated that the band at 1070 cm^{-1} becomes almost unchanged for the SBA15-cal sample compared to SBA15. These new absorption bands between 1150-1300 cm^{-1} are related to vibration modes of P=O bonds or different PO$_x$ metaphosphate units.[3-5] Particularly peaks at 1190 and 1255 in the spectrum of SBA15[P]-cal, which are very visible in SBA15[P]-cal, correspond to symmetric stretching vibrations of the metaphosphate units and asymmetric stretching modes of P=O bonds, respectively. Upon heat treatment, the positions of these peaks are known to change progressively to higher wave numbers. The new peak on 544 cm^{−1} on the spectrum SBA15[P]-cal can be assigned to assigned to harmonic bending vibration of O=P–O linkages.

Gas Adsorption Analaysis

The adsorption isotherms of the samples in Figure 2, these questions could be addressed as follows. The isotherms of SBA15[P]-sw and SBA15[P]-cal samples clearly show delayed desorption, indicating the presence of pore constrictions or plugs in the mesopores of these samples. The latter is possibly caused by residual phosphate ester and phosphonic acid groups within the mesopores in the case of SBA15[P]-sw and by metaphosphates in the case of SBA15[P]-cal. It is also worth noting that these two materials have showed higher adsorption in the lower relative pressure, indicating large monolayer coverage of nitrogen compared to sample SBA15-sw. This indicates the presence of a larger amount of micropores in the former samples than the latter. This further explains why the former samples have higher BET surface area that the latter as the BET surface area is calculated from the adsorption data for monolayer coverage by using the linear form of BET isotherm equation (x/[a(1-x)] vs. x where x = p/p$_s$) for mesoporous materials. If we separate the monolayer part from adsorption isotherm, we clearly see that samples SBA15[P]-sw and SBA15[P]-cal have higher monolayer adsorption, and consequently, larger surface areas. On the other hand the amount of micropores in the SBA15 sample is very low

possibly due to the presence of large fraction of residual P123 template remaining in its channels. This

is expected to give higher surface areas to the former compared to the latter.

On the other hand, the pore volume values are higher for SBA-15 especially compared to

SBA15^P-cal. As can be seen in Fig. 2 again, the total adsorption of nitrogen up to relative pressure x =

p/p$_s$ of ~0.98 in SBA15-sw is higher or about equal to that SBA15^P-sw and SBA15^P-cal samples. It is

worth noting that the total pore volume is calculated from the adsorbate volume at relative pressure x =

p/p$_s$ ca. 0.98 (p$_s$ is saturation pressure), where micropores and mesopores are filled-up. Furthermore, the

isotherms of SBA15^P-sw and SBA15^P-cal samples show delayed desorption and plugged pores while

that for SBA15-sw does not. This is expected to decrease the pore volume of these samples.

Figure S8 shows the gas adsorption isotherms of SBA15^P samples synthesized using lower

TEOS:P123^P ratio after solvent extraction. This experiment has allowed us to investigate the possibility

of pore constriction by the higher relative ratio of TEOS with respect to P123^P. The results indicate that

these samples also showed significant delayed desorption as the ones with higher TEOS/P123^P ratio.

Therefore, it can be concluded that the formation of plugs and constriction in the mesopores is not

caused by the TEOS amount but rather by the possible formation of phosphonic acids and phosphate

esters in the mesopores of samples synthesized from P123^P.

Table S1. Structural data of mesoporous materials.

Sample	Surface Area (m^2/g) [a]	Pore Volume (cm^3/g) [b]	Pore Volume (cm^3/g) [c]	Major Pore Diameter (nm) [d]	Small Pore Diameter (nm) [e]	Unit Cell (nm) [f]
SBA15^P-sw	804	0.63	0.27	8.53	2.28	11.5
SBA15^P-cal	717	0.53	0.21	8.52	2.28	10.3
SBA15-sw	428	0.68	0.09	7.97	NA	8.90

[a] BET surface area calculated from 0.05-0.2 range. [b] Single-point pore volume (total volume of small pores, primary mesopores and some textural porosity). [c] Pore volume of pores below 6 nm for interconnecting and complementary pores calculated by integration of pore size distribution up to 6 nm. [d] Pore diameter calculated with KJS method. [e] Maximum of small, complementary pores. [f] Unit cell calculated with P6mm hexagonal structure with $a_o = 2d_{100}/3^{1/2}$ (Å).

Table S2. Phosphorus content obtained by elemental analysis for phosphonated mesostructured and mesoporous samples.

Sample name	Content of Phosphorus
SBA-15^P Unextracted	916 ppm
SBA-15^P-cal	0.15 %
SBA-15^P-sw	510 ppm
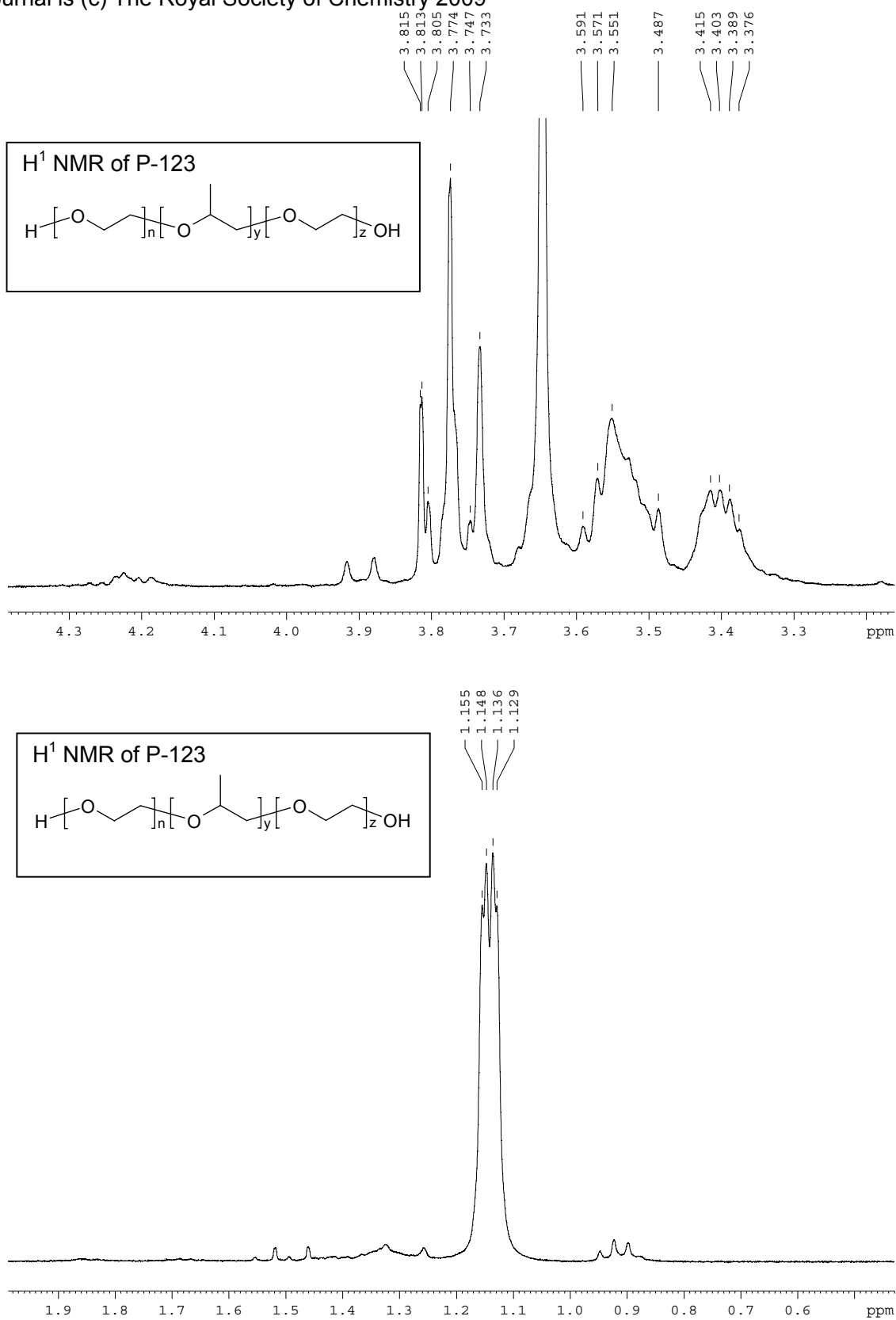
Figure S1. ^{1}H NMR spectra of Pluronic P123 triblock copolymer template.

10.448

7.939
7.273
7.270

5.613

3.815
3.813
3.805
3.774
3.747
3.733
3.591
3.571
3.551
3.487
3.415
3.403
3.389
3.376

1.155
1.148
1.136
1.129

H^1 NMR of Product

10   9   8   7   6   5   4   3   2   1   ppm
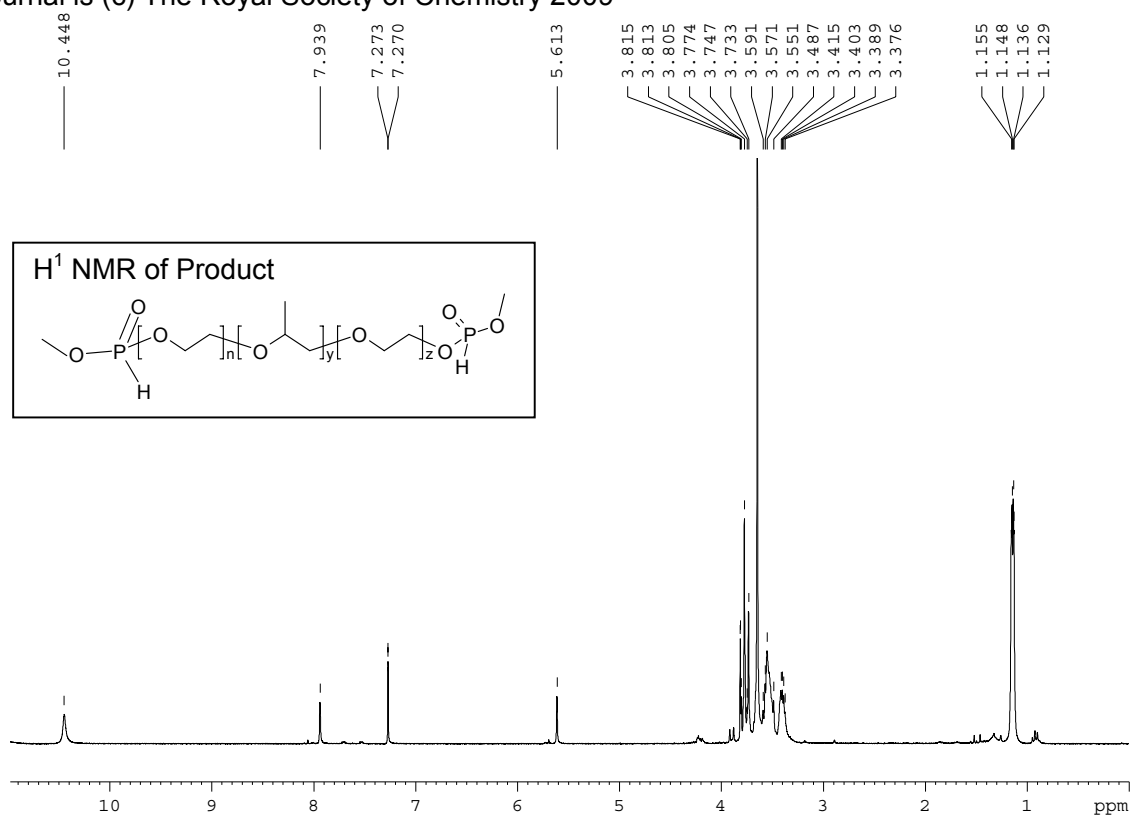
04-29-08 RF P-123+DMP Distillate

7.913
7.912
7.272
7.270

5.587
4.032
4.030
3.992
3.990
3.787
3.786
3.748
3.746
3.538
3.536
3.524
3.522
3.498
3.496
3.488
3.486
3.450
3.448
2.937
2.861

10   9   8   7   6   5   4   3   2   1   0   ppm

11
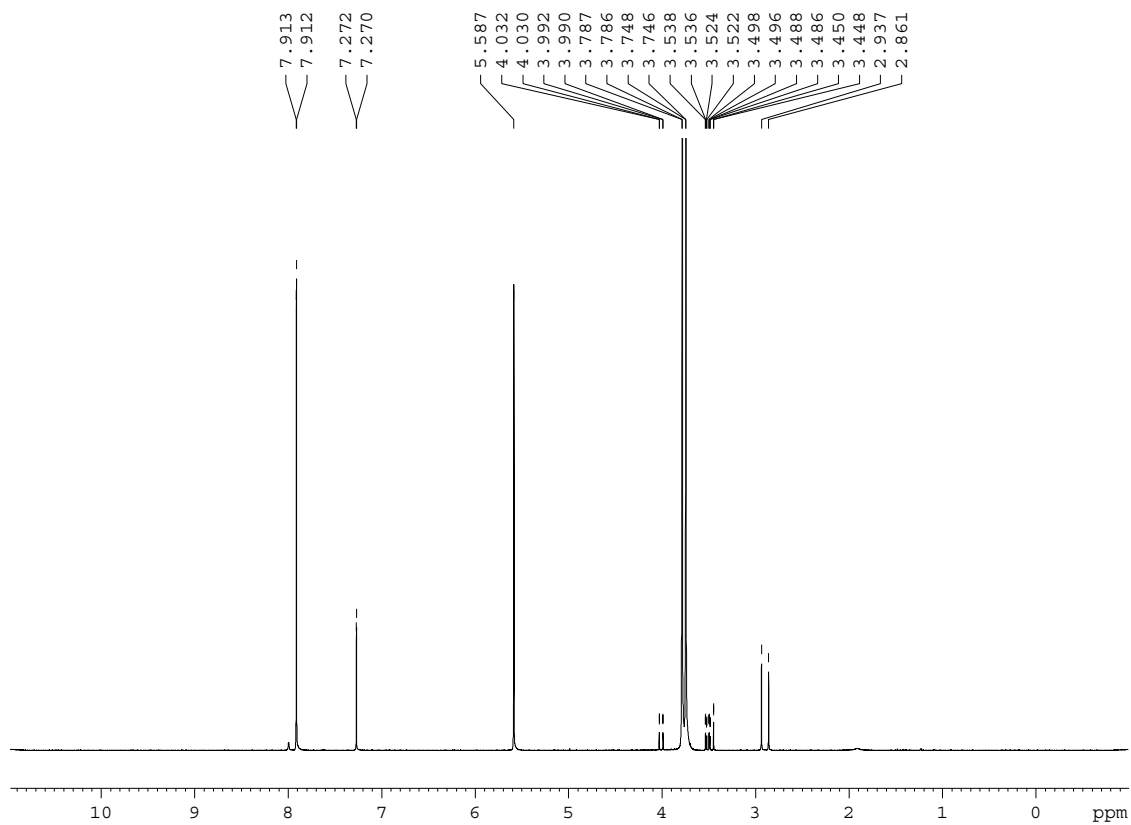
Figure S2. ^{1}H NMR spectra of phosphonated pluronics, P123^P triblock copolymer template.
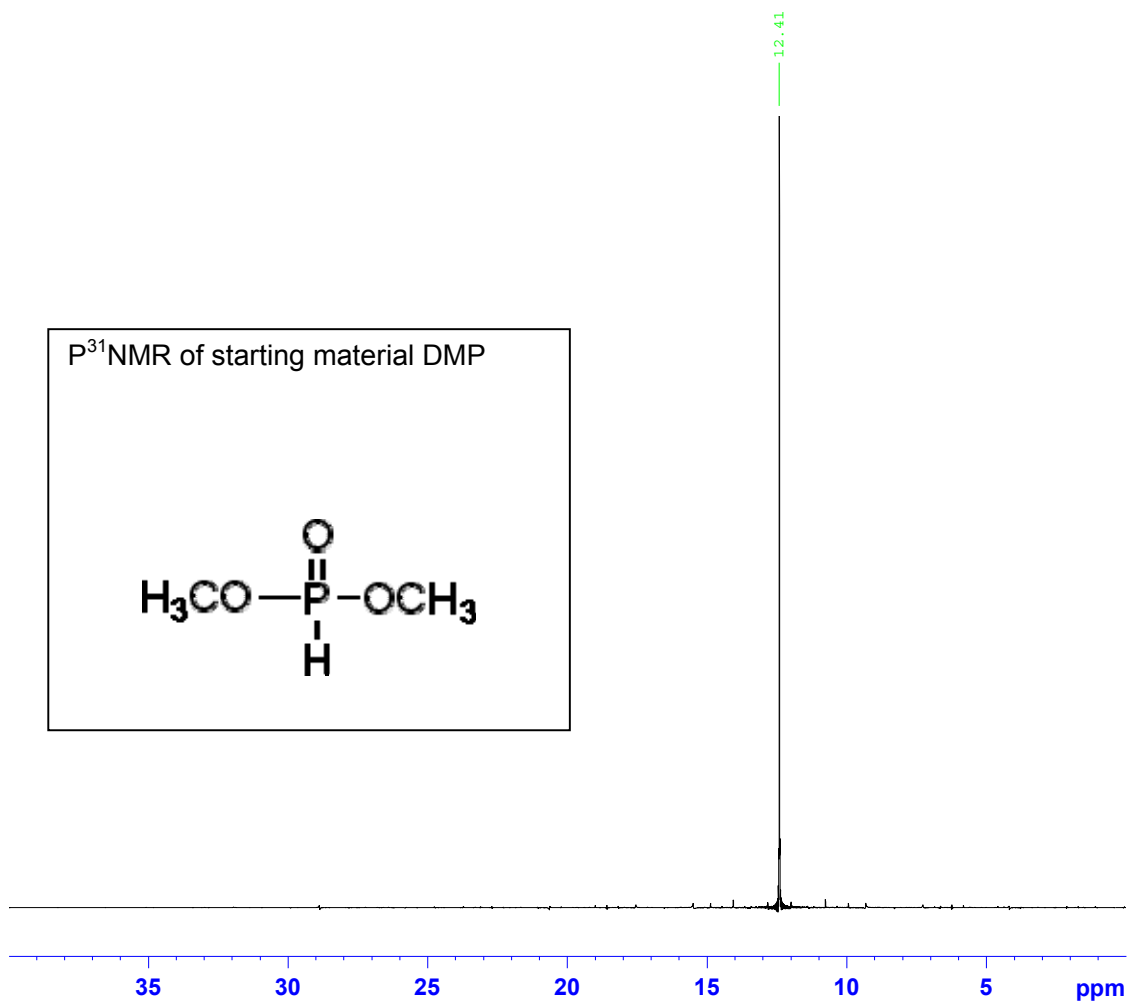
Figure S3. ^{31}P NMR spectrum dimethyl phosphite, DMP.
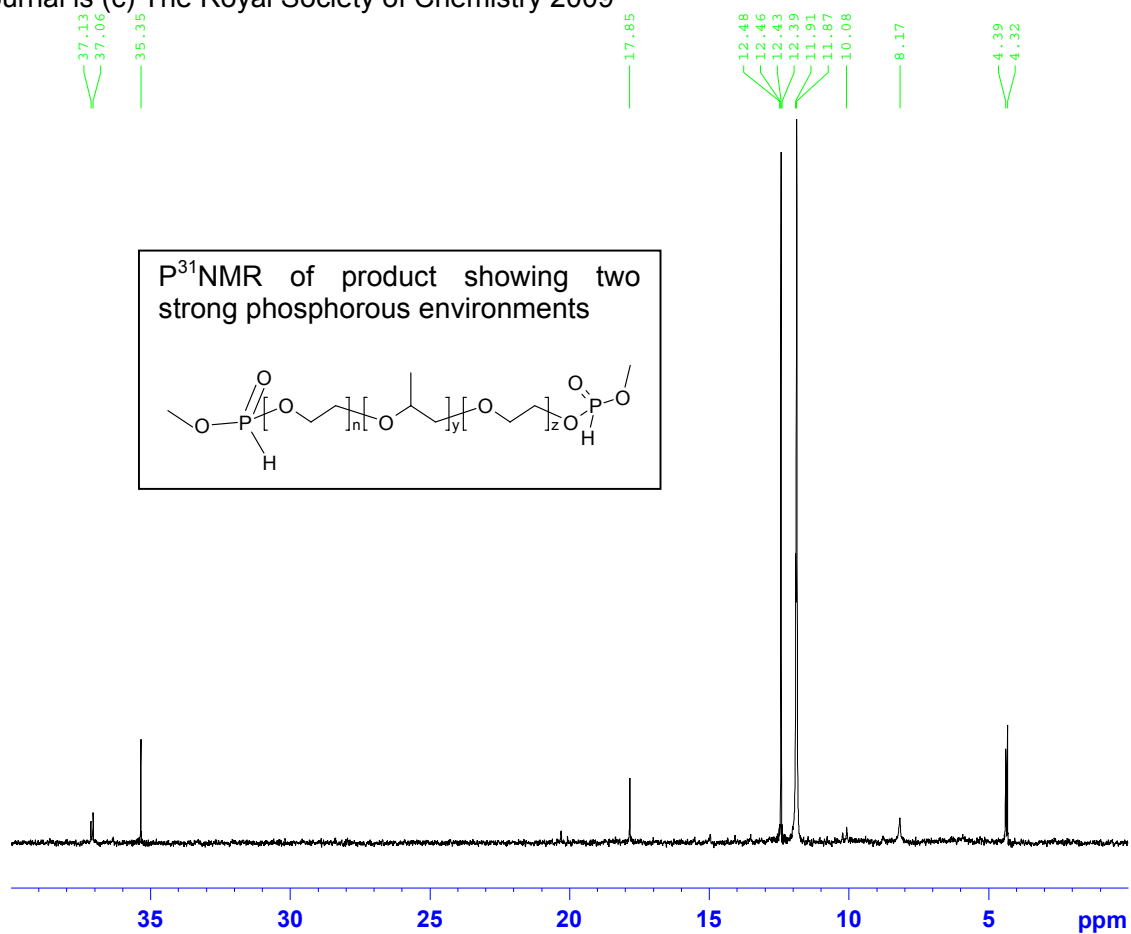
Figure S4. ^{31}P NMR spectrum phosphonated pluronic, P123^P.
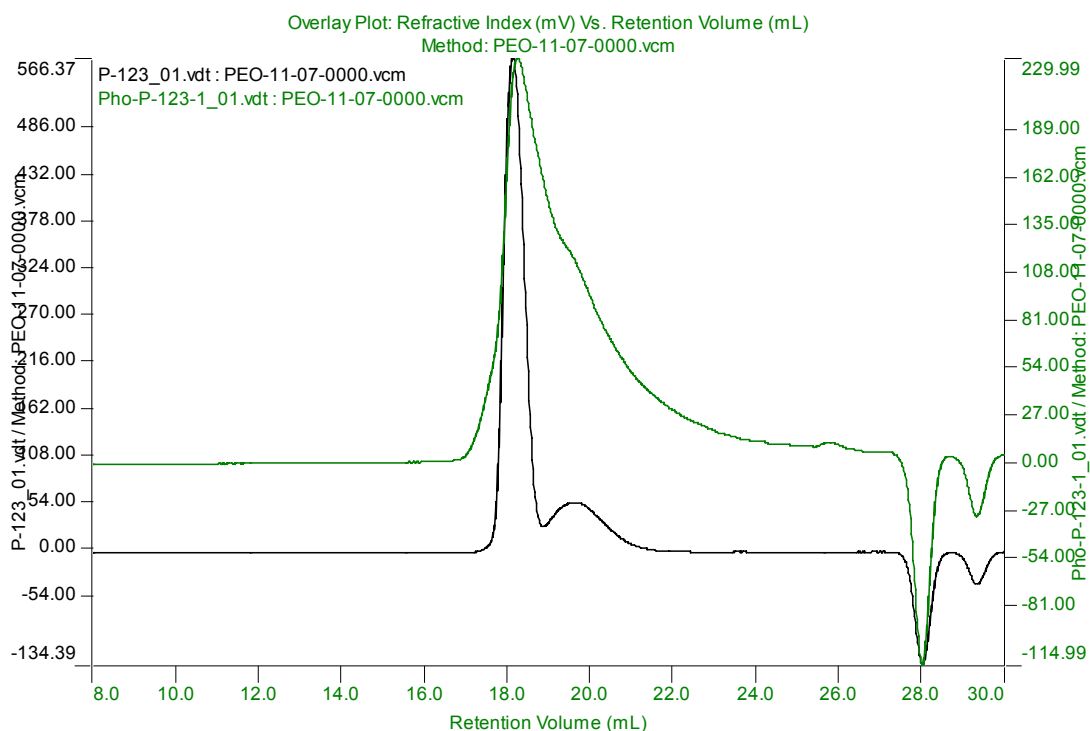
Figure S5. Size exclusion chromatography (SEC) of P123 (in black color) and P123[P] (or P123 after phosphorylation) (in green color). The black (lower) trace is the starting P-123, which has two fractions with different molecular weights, the right one being of lower molecular weight. The green (upper) trace is the phosphorylated derivative and it is obvious that some chemical transformation has occurred on it, since the shape is different. Based on previous reports of analogous samples[1] and based on the elution time of the sample as well as the signals in the NMR spectra (see above), a substantial part of the original P123 polymer is indeed phosphorylated.

14
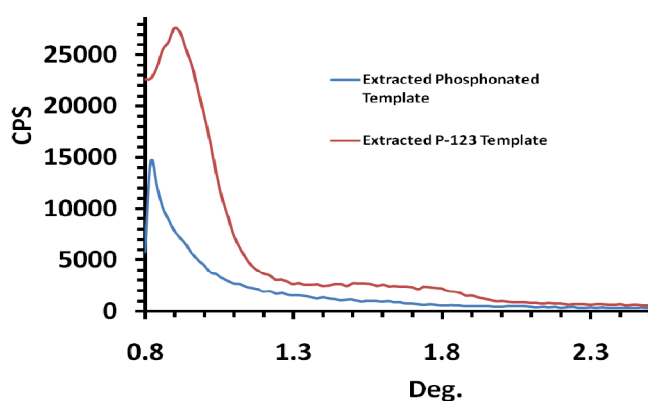
Figure S6. Power X-ray diffraction (XRD) patterns of solvent washed, SBA15^P-sw and SBA15,

samples.

(A) SBA15^P-sw
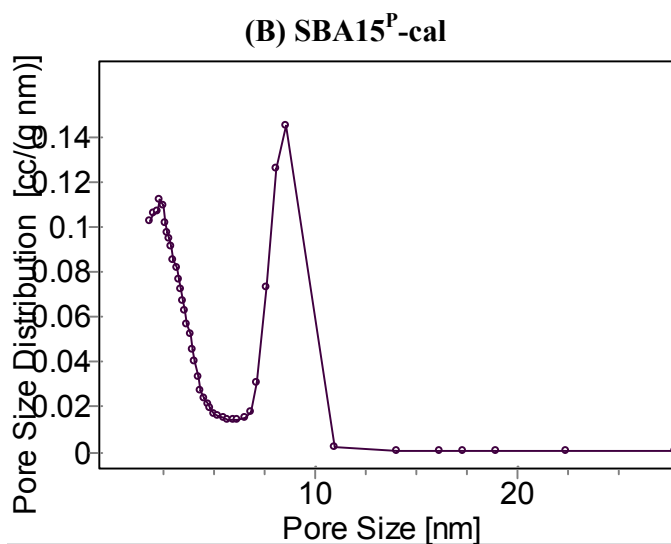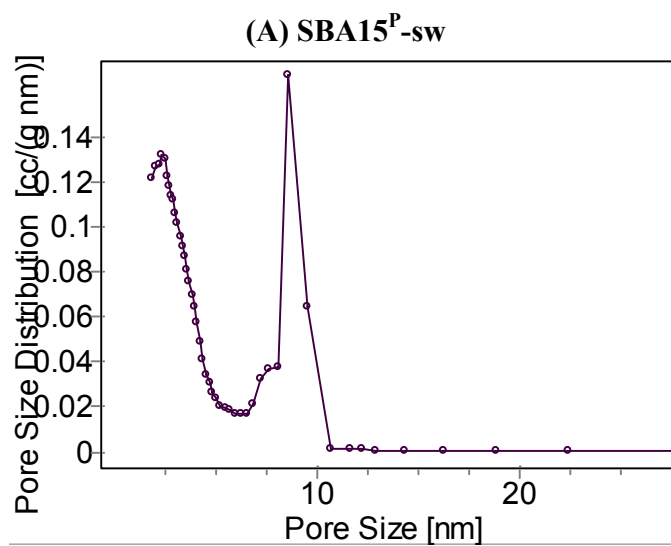
(B) SBA15^P-cal
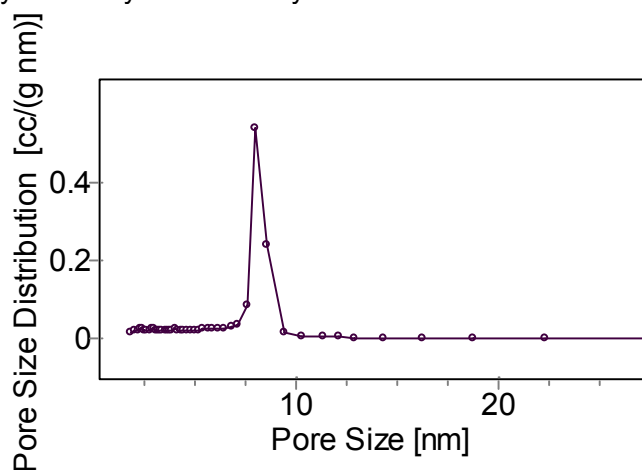
(C) SBA15-sw

Figure S7. Pore size distribution of template extracted samples (A) SBA15^P-sw, (B) SBA15^P-cal, and (C) SBA15.
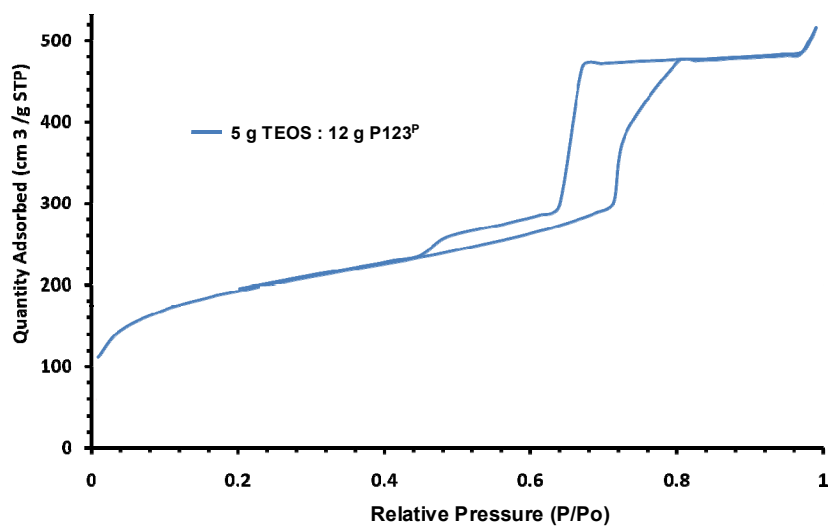

Figure S8. Adsorption isotherms for phosphonated mesoporous materials synthesized with lower TEOS/P123^P ratio after solvent extraction.
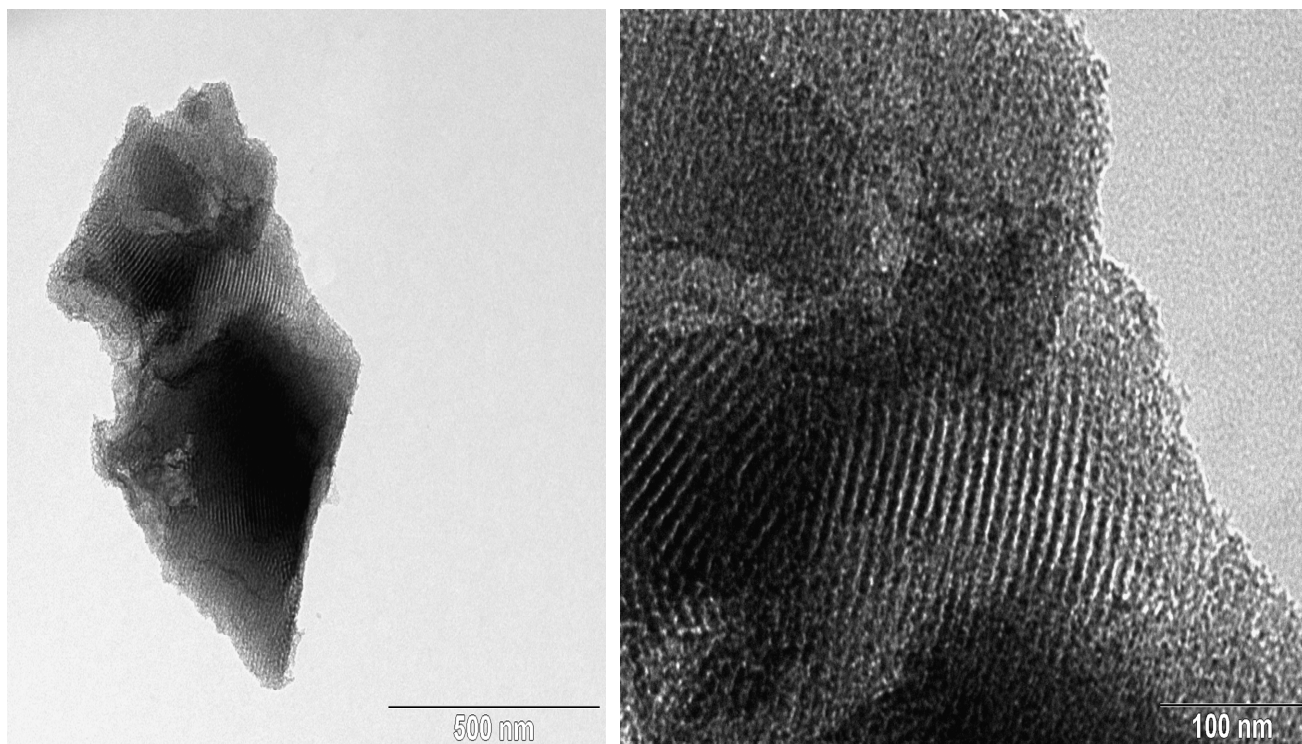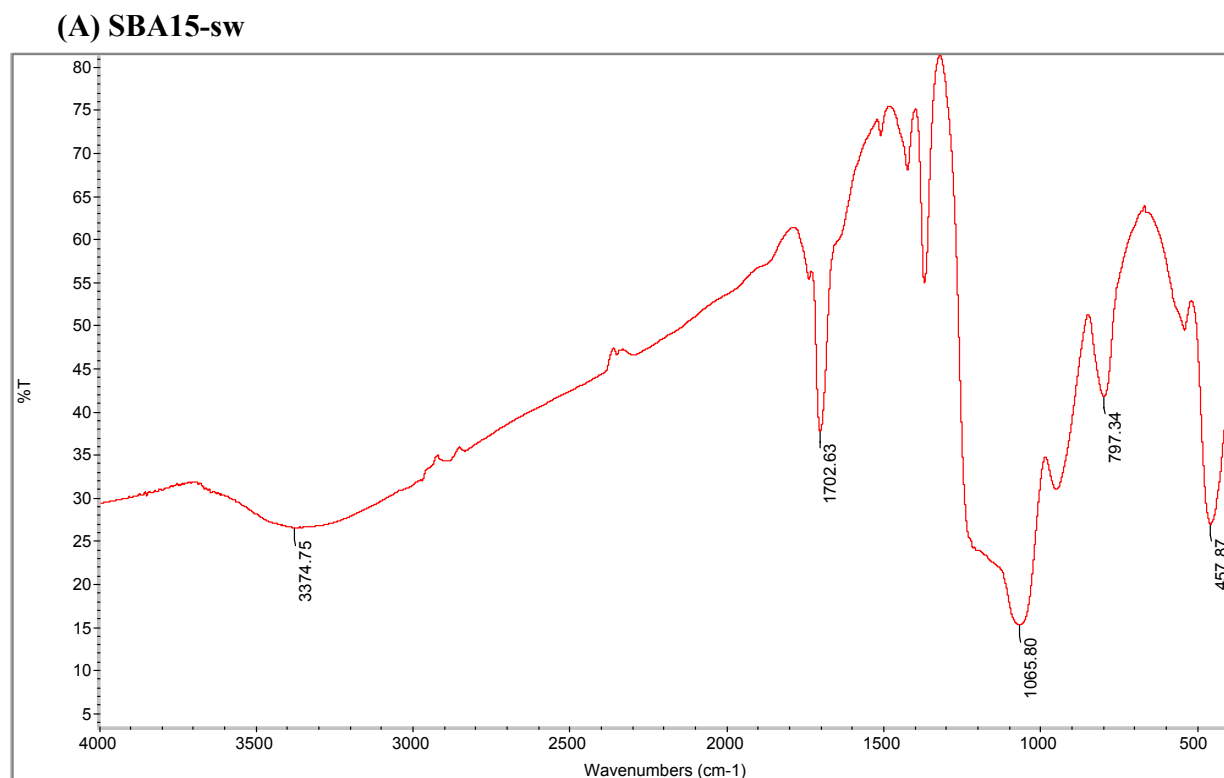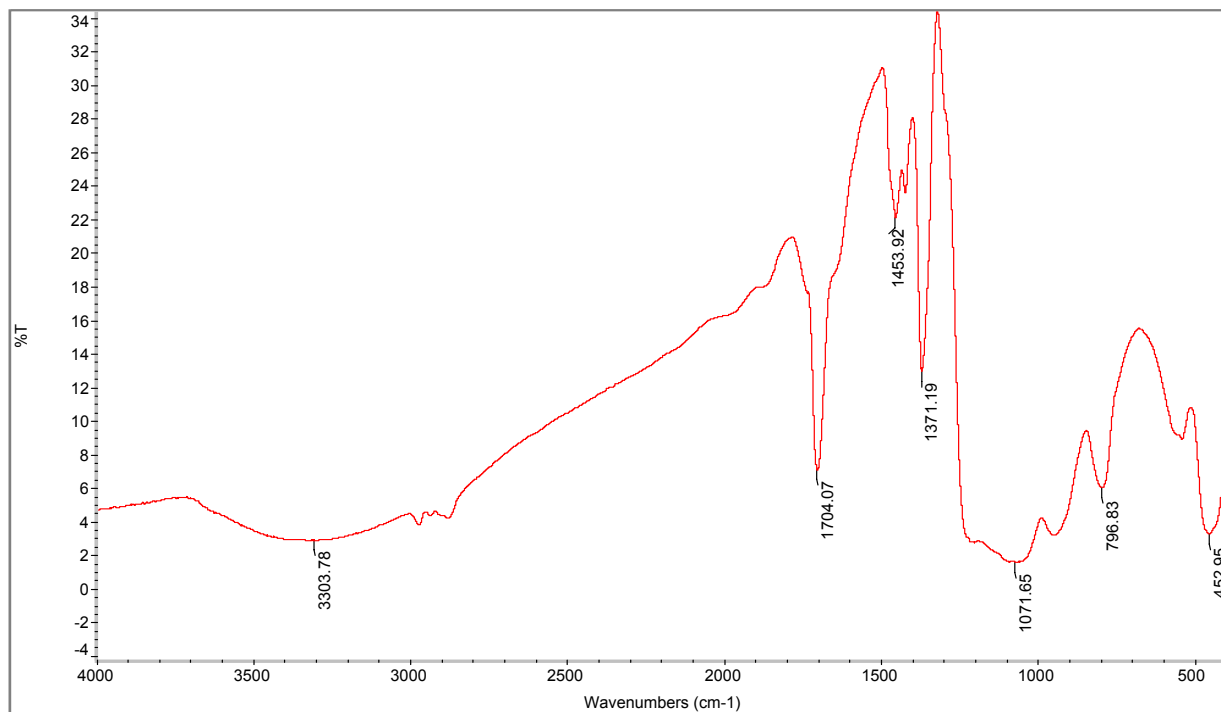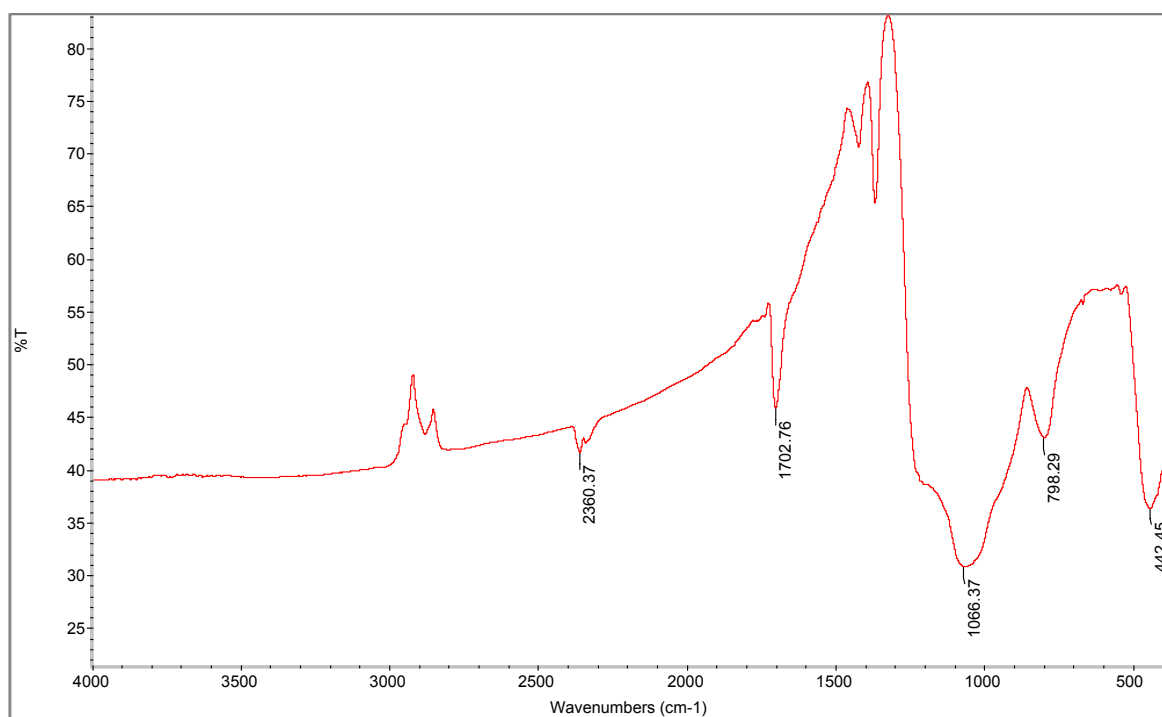
Figure S9. TEM images of mesoporous silica, SBA15^P-sw synthesized from phosphonated template. The images show that mesoporous channels extend through the entire material leaving a uniform network of hexagonal packed channels.

(A) SBA15-sw

(B) SBA15^P-sw

(C) SBA15-Cal
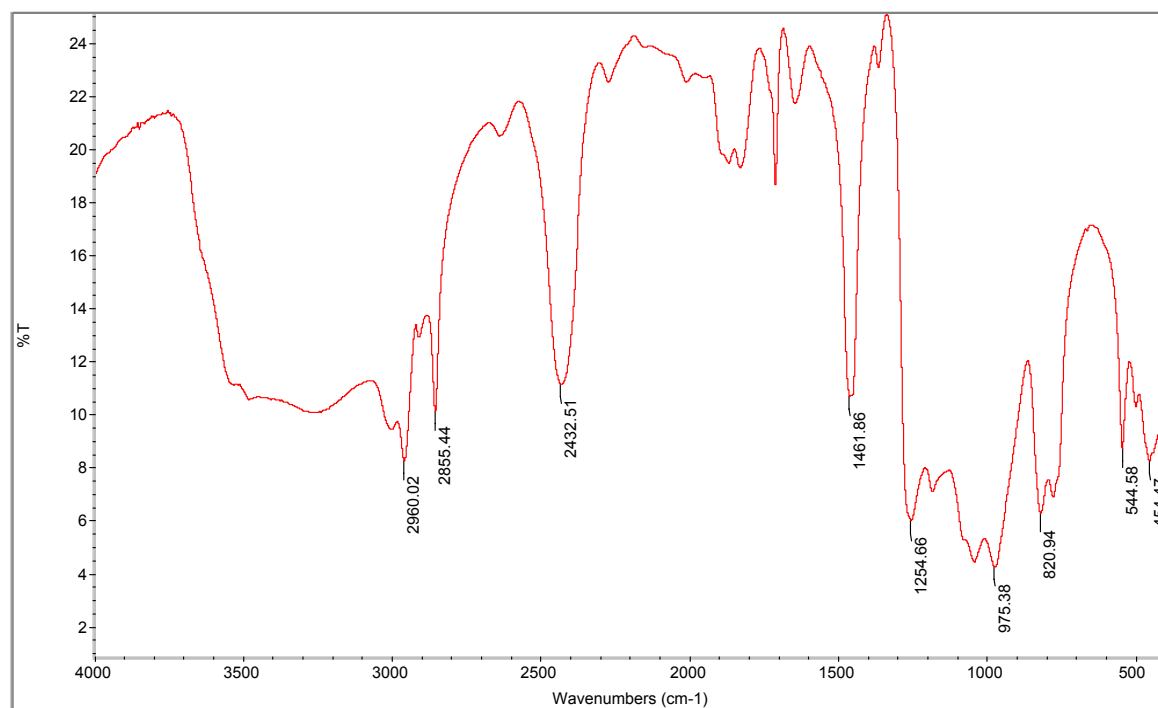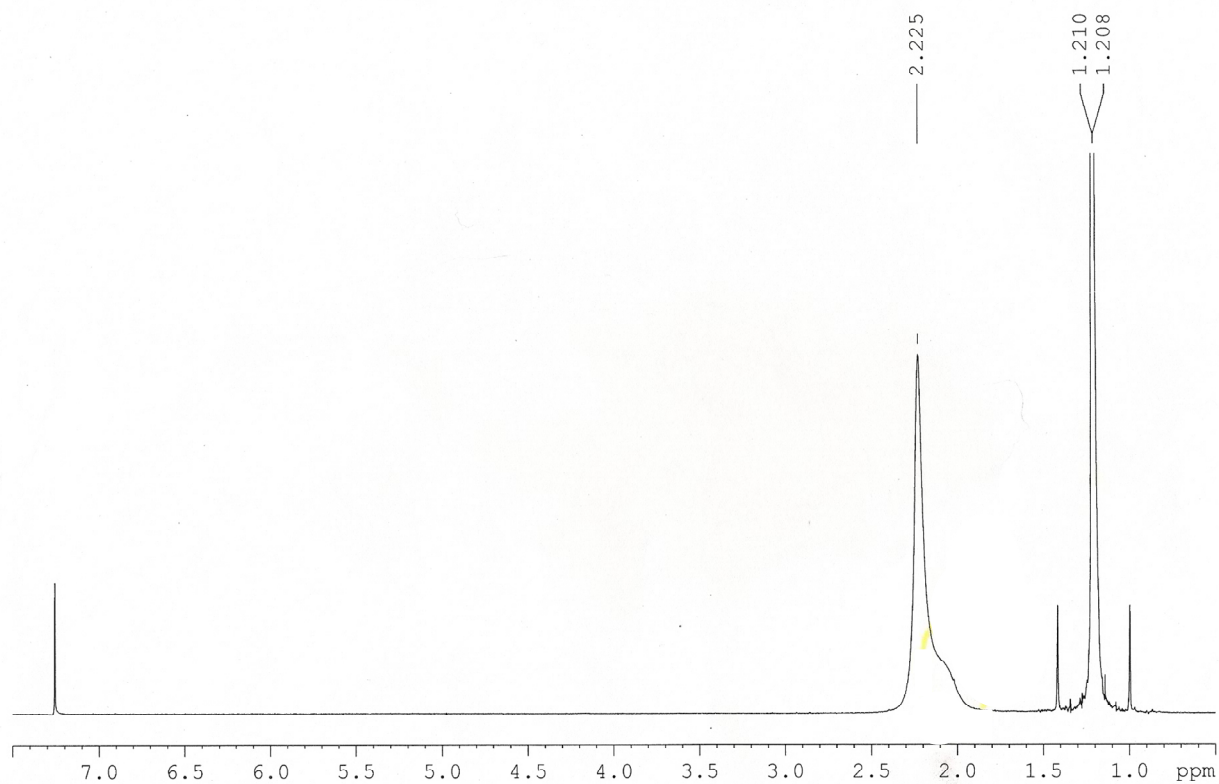
(D) SBA15^{P}cal

Figure S10. FT-IR spectra of SBA15 sample after (A) solvent washing (SBA15-sw) and (B) calcination (SBA15-cal); and SBA15^P sample after (C) solvent washing (SBA15^P-sw) and (D) calcination (SBA15^P-cal).

(A)

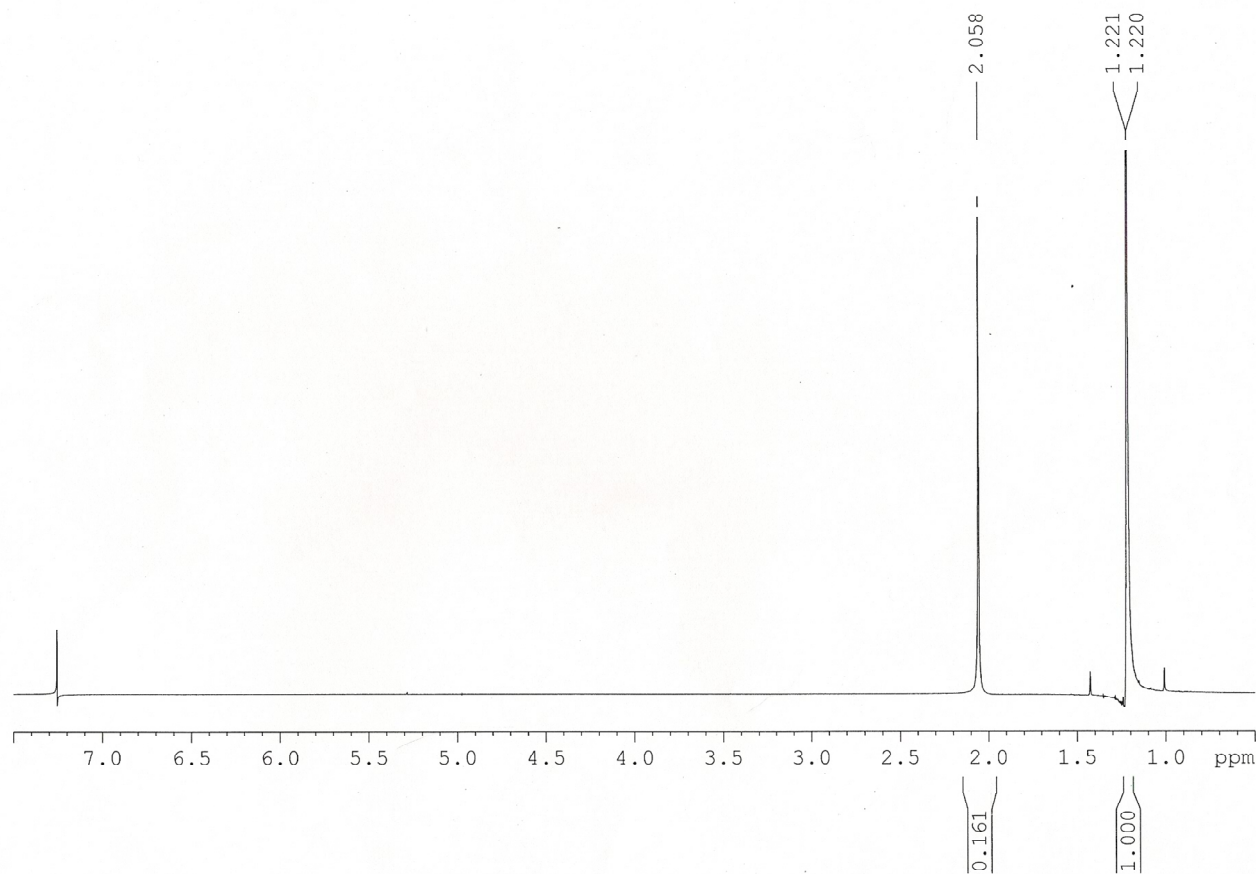12-01-08 RF P123 Solvent Washed

(B)

12-01-08 RF Solvent Washed PN

(C)

12-01-08 RF control Pinacol

Figure S11. Reaction mixture of a pinacole-pinacolone rearrangement reaction catalyzed by mesoporous catalysts synthesized from (A) P123 and (B) P123^P. (C) NMR spectrum of a pure reactant, pinacole.

Figure S12. ^{1}H NMR for benzopinacol and peak assignments, ^{1}H NMR (CDCl$_3$): δ 3.02 ppm (B: -OH)

and δ 7.45 – 6.98 (A: Ar-H). (Spectrum obtained from Sigma-Aldrich with permission).
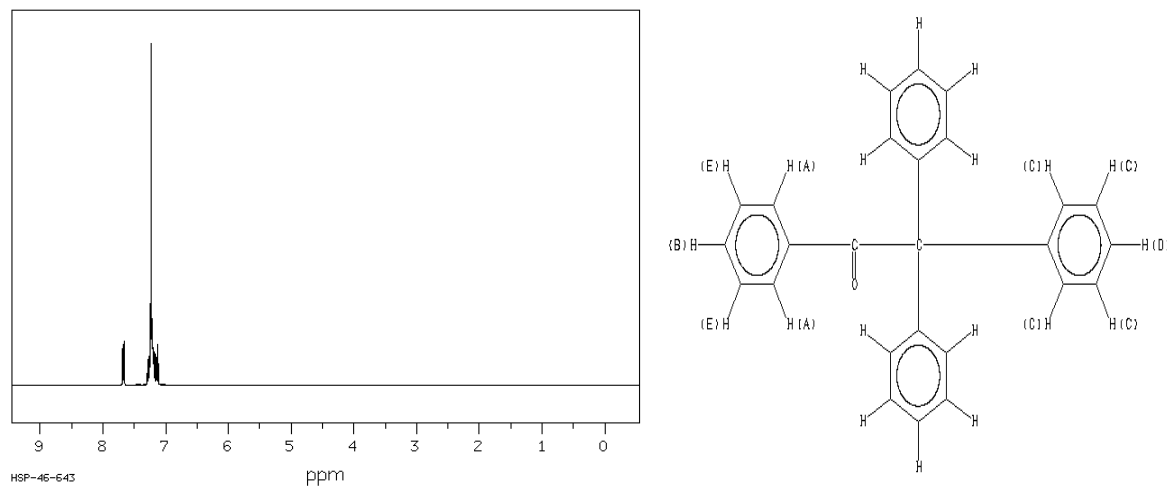
Figure S13. ^{1}H NMR for benzopinacolone and peak assignments, δ 7.68 (A: Ar-H) and δ 7.28 (B: Ar-

H), δ 7.23 (C: Ar-H), δ 7.21 (D: Ar-H), and δ 7.14 (E: Ar-H). (Spectrum obtained Sigma-Aldrich with

permission).

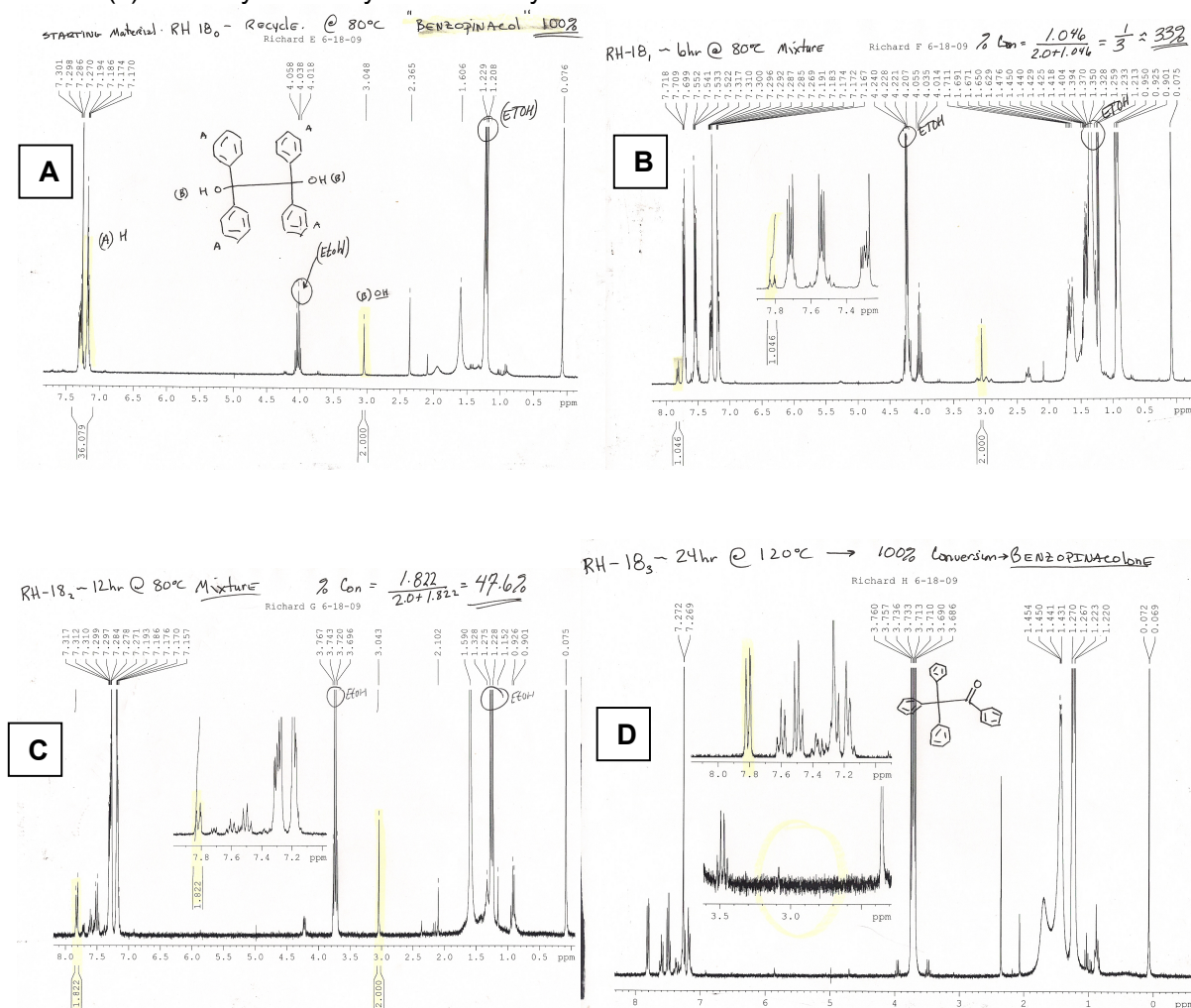**Figure S14.** ^{1}H NMR for data tabulated in Table 1 for the 1st recycle run of material which shows transformation of benzopinacol to benzopinacolone. (A) 100% starting material benzopinacol (B) 33% benzopinacolone (C) 48% benzopinacolone (D) 100% benzopinacolone.

References

1. I. Gitsov, F. E. Johnson, *J. Poly. Sci., Part A* 2008, **46**, 4130-4139.

2. D. Zhao, J. Feng, Q. Huo, N. Melosh, G. H. Fredrickson, B. F. Chmelka, G. D. Stucky, *Science* 1998, **279***, 548-551.

3. R. M. Almieda, J. D. Mackenzie, *J. Non-Cryst. Solids* 1980, **40**, 535-548.

4. K. V. Shah, M. Goswami, M. N. Deo, A. Sarkar, S. Manikandan, V. K. Shrikhande, G. P. Kothiyal, *Bull. Mater. Sci*., 2006, **29**, 43-48.

5. E. W. Shi, J. S. Han, M. Jang, S.-H. Min, J. K. Park, R. M. Rowell, *Environ. Sci. Technol*. 2004, **38**, 912-917.